

Reactive gaseous mercury formation in the North Pacific Ocean's marine boundary layer: A potential role of halogen chemistry

Fabien J. G. Laurier, Robert P. Mason, and Lindsay Whalin

Chesapeake Biological Laboratory, University of Maryland, Solomons, Maryland, USA

Shungo Kato

Department of Applied Chemistry, Tokyo Metropolitan University, Tokyo, Japan

Received 21 March 2003; revised 9 June 2003; accepted 25 June 2003; published 4 September 2003.

[1] Reactive gaseous mercury (RGHg), atmospheric elemental mercury (Hg^0), and ozone (O_3) along with other ancillary parameters have been measured simultaneously in the marine boundary layer (MBL) over the North Pacific Ocean during the 2002-IOC cruise between Osaka, Japan, and Honolulu, Hawaii. Atmospheric Hg^0 concentrations varied from 1.6 to 4.7 ng m^{-3} with an average of 2.5 ng m^{-3} and did show significant variations along the cruise track with a slight diel cycle in Hg^0 concentrations. RGHg concentrations varied from 0.15 to 92.4 pg m^{-3} with an average of 9.5 pg m^{-3} . The data strongly suggest photochemical in situ formation of RGHg with increasing concentrations in the tropical regions concomitant to a dramatic decrease in O_3 (from over 50 to less than 5 ppbv). A distinct diurnal variation in RGHg concentrations with maxima at midday suggests a photochemically driven oxidation of marine boundary layer Hg^0 . In the tropical area, enhanced RGHg formation and daily variation in O_3 could both be related to reactive halogen chemistry. Flux calculations also emphasize the role of the tropical marine boundary layer in mercury cycling over the North Pacific Ocean. **INDEX TERMS:** 0312 Atmospheric Composition and Structure: Air/sea constituent fluxes (3339, 4504); 0330 Atmospheric Composition and Structure: Geochemical cycles; 1065 Geochemistry: Trace elements (3670); 4227 Oceanography: General: Diurnal, seasonal, and annual cycles; **KEYWORDS:** reactive gaseous mercury, marine boundary layer, reactive halogen chemistry

Citation: Laurier, F. J. G., R. P. Mason, L. Whalin, and S. Kato, Reactive gaseous mercury formation in the North Pacific Ocean's marine boundary layer: A potential role of halogen chemistry, *J. Geophys. Res.*, 108(D17), 4529, doi:10.1029/2003JD003625, 2003.

1. Introduction

[2] Atmospheric deposition is the dominant source of mercury (Hg) to most remote water bodies [Nriagu and Pacyna, 1988; Mason *et al.*, 1994] and its understanding is fundamental, because of the ability of mercury to bioaccumulate through all levels of the food chain. Global Hg models have identified wet and dry particle deposition and evasion of dissolved gaseous Hg (DGHg) from the ocean as key controls over global Hg cycling [Mason *et al.*, 1994; Hudson *et al.*, 1995; Lamborg *et al.*, 1999; Shia *et al.*, 1999]. Dissolved gaseous mercury (DGHg) exists both as elemental Hg (Hg^0) and dimethylmercury (DMHg) [Kim and Fitzgerald, 1988; Mason *et al.*, 1995; Cossa *et al.*, 1997; Lamborg *et al.*, 1999] with Hg^0 being the dominant form of DGHg in the upper ocean. Studies that have focused on air-sea exchange for both Atlantic [Mason *et al.*, 1995; Mason and Sullivan, 1999; Lamborg *et al.*, 1999] and Pacific Oceans [Kim and Fitzgerald, 1988; Mason and Fitzgerald, 1993] have suggested that the

estimated evasion rates for Hg from the ocean substantially exceed the current deposition estimates from both atmospheric and riverine inputs. One potential reason for this lack of balance is that current measurements of DGHg come from a limited number of studies and thus do not accurately represent the seasonal average concentration or the potential variability in concentration. Another reason could be that not all the potential sources of Hg to the ocean have been properly quantified. While Hg evasion from both the ocean and the terrestrial environment is considered mainly in the form of Hg^0 , deposition is characterized by three different types of atmospheric species: gaseous Hg^0 , gaseous ionic divalent Hg or reactive gaseous mercury (RGHg), and particulate Hg (Hg-P) [Lindberg and Stratton, 1998; Schroeder and Munthe, 1998; Sheu and Mason, 2001]. Hg^0 and RGHg are both known to be emitted from industrial sources [Porcella *et al.*, 1997] and to contribute to atmospheric deposition [Lindberg and Stratton, 1998; Bullock, 2000; Sheu *et al.*, 2002]. Although RGHg species represent only a few percent of the total gaseous mercury, their high solubility, $1.4 \times 10^6 \text{ M atm}^{-1}$ at 25°C, compared to Hg^0 , 0.11 M atm^{-1} at 25°C [Lin and Pehkonen, 1999a], and their high dry

deposition velocities which is of 5–10 times greater than Hg^0 [Shia *et al.*, 1999; Bullock, 2000] make their removal more efficient than the other atmospheric species.

[3] Recent global Hg models have incorporated the dry deposition of RGHg derived from point source emissions, showing that RGHg deposition can have an impact on a local/regional scale [Shia *et al.*, 1999; Bullock *et al.*, 1997; Bullock, 2000; Pai *et al.*, 1997; Xu *et al.*, 2000]. However, these models, have not always taken into account the production and the deposition of RGHg formed in remote places by all the potential gas phase and/or heterogeneous reactions [Pleijel and Munthe, 1995; Lin and Pehkonen, 1998] such as oxidation of Hg^0 by halogens radicals [Lin and Pehkonen, 1999b; Ariya *et al.*, 2002]. The imbalance between evasion and deposition estimates for the ocean suggests a removal of Hg^0 more likely by oxidation/deposition, as shown by recent studies which support the production of RGHg in the marine boundary layer [Guentzel *et al.*, 2001; Hedgecock and Pirrone, 2001; Mason *et al.*, 2001].

[4] Schroeder *et al.* [1998] showed a depletion of total gaseous mercury in the atmosphere during Arctic polar sunrise (Alert, Canada) with concomitant ozone depletion, suggesting Hg^0 oxidation and thus RGHg formation. Laboratory kinetic experiments and mechanistic data suggest that the chain reaction leading to ozone depletion in the Arctic is initiated by halogen radicals (more likely atomic bromine) through the photolysis of gas phase halogen compounds [Barrie *et al.*, 1988; Finlayson-Pitts *et al.*, 1990; Mozurkewich, 1995; Platt and Moortgat, 1999; Foster *et al.*, 2001; Bottenheim *et al.*, 2002; Spicer *et al.*, 2002]. The source of those radicals is believed to be oxidation of halogens in sea-salt aerosol, snow, and frozen ocean surface [McConnell *et al.*, 1992; Barrie and Platt, 1997; Foster *et al.*, 2001]. In Arctic environment, Hg^0 oxidation and production of RGHg seems to be attributed to the same photochemical mechanisms [Lu *et al.*, 2001; Ebinghaus *et al.*, 2002; Lindberg *et al.*, 2002]. In the marine boundary layer, chlorine and bromine can also be released into gas-phase by heterogeneous reactions on sea-salt aerosols [Fickert *et al.*, 1999; Vogt *et al.*, 1996; Hirokawa *et al.*, 1998; Ayers *et al.*, 1999; Knipping *et al.*, 2000]. Adsorption of HOBr on wet sea salt (at humidity above the deliquescence point) leads to release of Br_2 and BrCl and which photolysis to produce Br atoms that provide additional photochemical ozone sink [Dickerson *et al.*, 1999; Sander *et al.*, 1999]. The presence of reactive halogen species in the marine boundary layer is supposed to play a role in Hg^0 oxidation and production of RGHg. This hypothesis is supported by modeling experiments and recent results obtained for the Mediterranean region [Hedgecock and Pirrone, 2001; Hedgecock *et al.*, 2003; Sprovieri *et al.*, 2003].

[5] In our study, all the measurements were obtained during the 2002 Intergovernmental Oceanographic Commission (IOC) cruise transect over the North Pacific Ocean. The aim of the 2002 IOC cruise was to identify the role of Southeast Asia dust atmospheric transport processes in delivering reactive trace elements and other materials to the surface ocean. Beside the influence of Southeast Asia dust deposition on mercury cycling in the North Pacific Ocean water, we focus in this study on in situ Hg^0 oxidation

and on the environmental parameters, which could influence RGHg formation.

2. Material and Method

2.1. Cruise Background

[6] The research proposed with the 2002 IOC cruise has, as its primary objective, examining the relationships between inputs, cycling and transport of a variety of biologically and geochemically significant trace elements (including Al, Fe, As, Sb, and Se) on a transect across the central and western North Pacific. The cruise track provided (Figure 1) the opportunity to collect air and seawater samples spanning a large range of dust deposition fluxes into a variety of hydrologically distinct biogeochemical zones. The cruise, on the RV *Melville* (Scripps Institute of Oceanography), started from Osaka, Japan ($34^\circ 65' \text{N}$, $135^\circ 42' \text{W}$), on May 1st 2002 and ended in Honolulu, Hawaii ($24^\circ 15' \text{N}$, $153^\circ 84' \text{E}$), on June 4th 2002.

[7] All the data reported here were collected aboard from $47^\circ 83' \text{N}$, $162^\circ 50' \text{W}$ to $22^\circ 75' \text{N}$, $158^\circ 00' \text{E}$ (Figure 1) during a three weeks sampling period (May 14th, May 30th) as the atmospheric mercury measurements obtained for the first week of the cruise were discarded due to instrumentation problems.

2.2. Sampling and Analytical Techniques

[8] Meteorological parameters, air temperature, relative humidity, barometric pressure, wind speed, and wind direction were measured by the RV *Melville*'s continuous underway data monitoring system with integration steps every 30 s. Atmospheric Hg^0 and RGHg measurements were performed using the Tekran mercury speciation unit, Tekran 1130 speciation unit coupled to Tekran 2537A analyzer (Tekran Inc., Toronto, Canada) described by Landis *et al.* [2002]. The precision of the instrument based on field comparisons of paired 1130 speciation unit exhibits a precision of 15% [Landis *et al.*, 2002]. The speciation unit was set up on the front of the ship at $\sim 15 \text{m}$ above sea level. Hg^0 was determined using a vapor-phase mercury analyzer (Model 2537A) which consists in two gold traps where mercury is consecutively adsorbed and then desorbed into a cold-vapor atomic fluorescence spectrometer [Bloom and Fitzgerald, 1988]. The Tekran model 1130 speciation unit was used for the RGHg measurements. The 1130 unit (sampling module) included a heated KCl-coated quartz annular denuder, a heated sampling line, a pump module, and a controller module. By integrating the analytical capabilities of the 2537A analyzer with the 1130 speciation unit, the controller module allows full control over sampling parameters (sample flow rate, sample duration, desorption temperature, etc.) for continuous measurement of both Hg^0 and RGHg at pg.m^{-3} concentrations. The speciation system was typically set up for a sampling time resolution of 5-min for Hg^0 and 2-h for RGHg. By pumping ambient air through the denuder, RGHg is adsorbed onto the KCl coated denuder while Hg^0 is quantified in the analyzer. After a 2-h sampling period, the denuder is heated to 500°C and RGHg is thermally decomposed into mercury-free air and analyzed as Hg^0 . The particulate mercury was collected on a downstream quartz fiber filter and was not analyzed. Ozone was measured using Thermo Environmental Instruments,

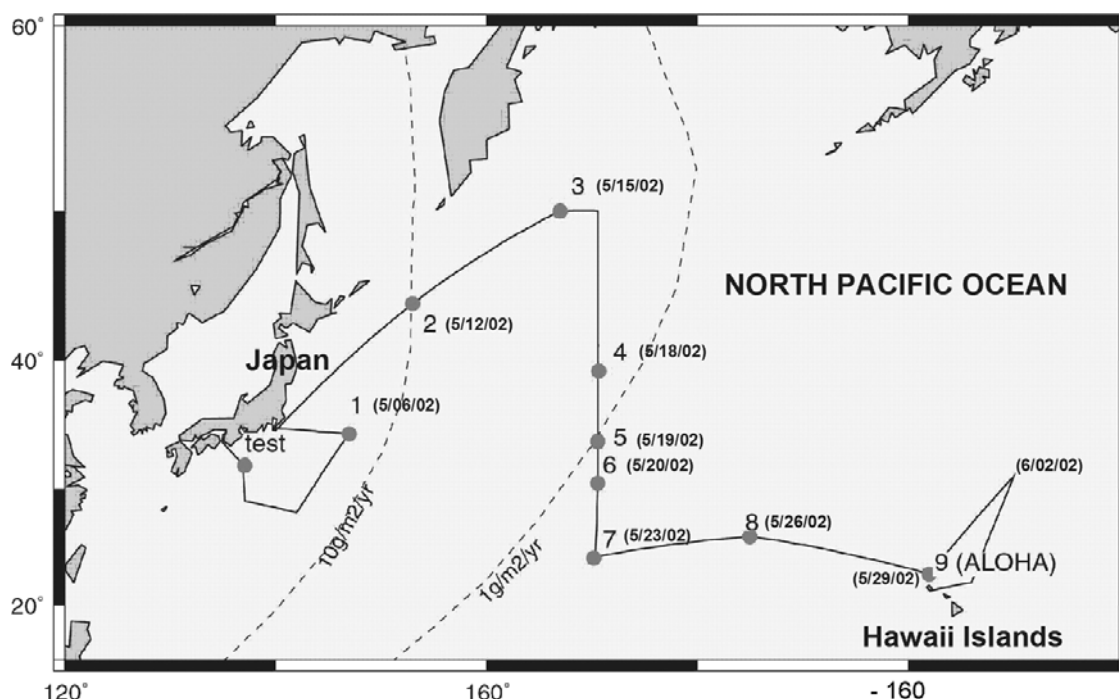


Figure 1. IOC 2002 Cruise Track Cook Expedition, Leg 23, [COOK23MV]. Chief scientist: Chris Measures; begin date/port: 01-May-02 Osaka, Japan ($34^{\circ}65'N$, $135^{\circ}42'W$); end date/port: 04-Jun-02 Honolulu, HI ($24^{\circ}15'N$, $153^{\circ}84'E$). The numbers from 1 to 9 and the relative dates correspond to the depth-profile sampling station with the “test” as a test station. The dashed lines represent the estimated Southeast Asian dust deposition.

Model 49C which was calibrated by an ozone standard generator (Model 49CPS). Carbon monoxide concentrations were obtained by IR absorption (Thermo Environ. Instrument 48C). The underway surface-water samples were collected using a “fish” sampler, which is a device pulled in the surface water beside the ship while it is moving forward with the inlet being away enough ($>5m$) to avoid the ship’s contamination. Water was pumped on board the ship into a laminar flow hood using a peristaltic pump through acid-cleaned tubing. The sample were collected in 2 l Teflon bottles and were processed on board immediately after collection, or at least within 3 hours after collection, in an onboard clean container; this sampling technique prevented the sample from contacting the ship environment. Sample collection and treatment were performed using ultraclean techniques. Polyethylene gloves were used for handling operations. All Teflon and plastic-ware had been acid washed (3 days in 50% HNO_3 , then 3 days in 10% HNO_3 at $50^{\circ}C$) and rinsed several times with Milli-Q[®] water prior to use. Cleaned Teflon bottles were filled with Milli-Q water, acidified with HCl (1% v/v) and stored in double polyethylene bags until use. The samples (unfiltered) were analyzed for dissolved gaseous mercury (DGHg). DGHg concentrations were measured using a Teflon bubbler head attachment that fitted directly onto the 2-L Teflon bottles. Samples were bubbled for 40-min at 500 ml min^{-1} with Hg-free argon in a laminar flow hood and the released DGHg was trapped on gold columns. Quantification, by cold-vapor atomic fluorescence spectrometry (CVAFS), was achieved by heating the gold trap in a stream of argon. The released Hg^0 vapor was analyzed by the atomic fluores-

cence detector [Bloom and Fitzgerald, 1988]. The sampling protocols and surface-water sampling device have been described by Cutter and Measures [1999] and a previous comparison study on DGHg measurements showed the integrity of the results [Mason *et al.*, 2001].

3. Results and Discussion

3.1. Ancillary Data

[9] In order to enhance the comparability of the data, the barometric pressure, air temperature, and relative humidity data presented in the Figure 2 correspond to a 2-hour integration, comparable to each RGHg measurement, of the 30-s step MET data. The data collected between May 14th and May 31st corresponded to two different geographical and hydrographical zones (Figures 1 and 2). The first zone, concerning the sampling period between May 14th and May 21st, can be mainly characterized by relatively cold to mild air temperatures due to the influence of the Subarctic gyre’s water mass and by low UV irradiation (maxima average of $\sim 45\text{ W/m}^2$) as a result of stormy weather conditions. The second zone, from May 22nd to May 31st, corresponded to the tropical waters (North Pacific subtropical gyres and Kuroshio current), characterized by warm temperatures and high UV irradiation (maxima average of $\sim 65\text{ W/m}^2$). The air temperature and the surface water temperature (data not shown) followed a very comparable trend. For both, the values increased from less than 5 degrees Celsius at the beginning of the sampling period and reached a threshold value of 25 degrees Celsius on May 22nd which corresponded to the tropical water. The varia-

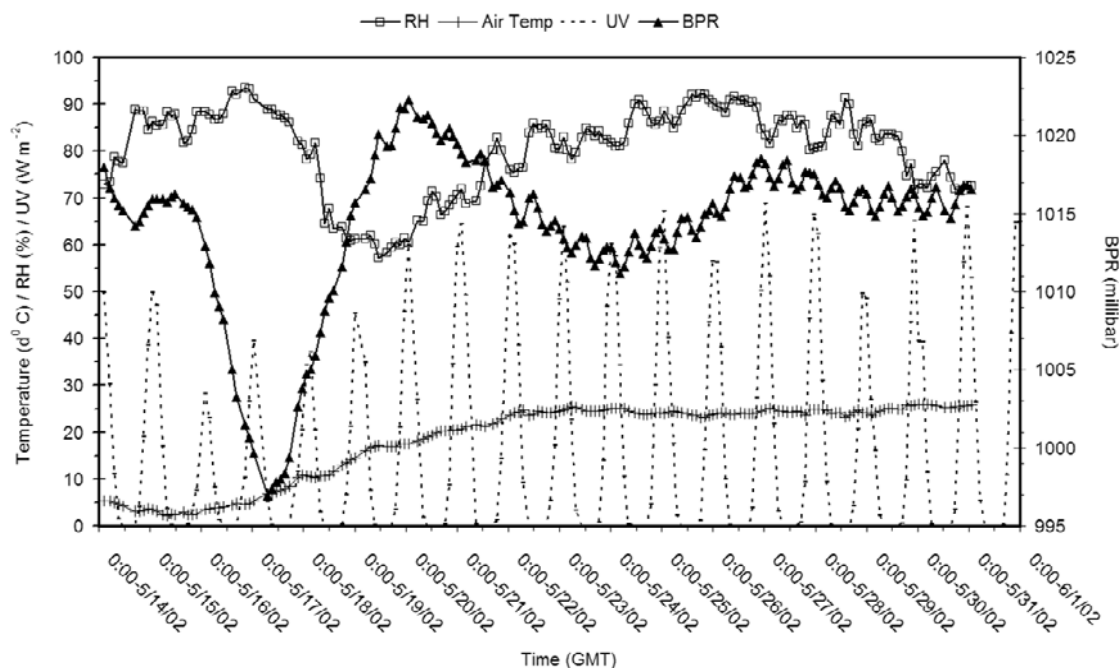


Figure 2. Ancillary atmospheric data (MET data) with RH (relative humidity, %), Air Temp (air temperature, degrees Celsius), UV and BPR (barometric pressure, mbars). The data correspond to a 2-hour step integration of the MET data. The time corresponded to Greenwich Mean Time (GMT).

tions observed for the relative humidity were due to different meteorological conditions. The low-pressure system observed within the first days of the cruise period was associated with cloudy conditions leading to a decrease of UV radiation and high relative humidity. The following high-pressure system was characterized by clear sky, higher UV radiation and lower relative humidity. At low latitudes, the meteorological conditions were typical of a tropical climate with mainly clear sky associated with low scattered cumulus, high UV, high temperatures and high relative humidity. However, although the tropical area displayed quite homogeneous meteorological conditions, significant differences in wind speed and in wet deposition as the cruise reached the Hawaiian Islands area (5 last days of the cruise, Figure 1), seemed to strongly influence the atmospheric mercury concentrations as discussed further (see sections 3.5 and 3.6). Consequently, we discussed the data in terms of three distinct temporal and spatial periods based mainly on the three distinct atmospheric mercury patterns (see section 3.3). No event of strong rain was reported during the cruise, although tropical rain showers were encountered during the latter part of the cruise.

3.2. Potential External Contaminations

[10] In order to determine whether there was local contamination coming from the exhaust stack gases of the boat and to assess the degree of impact of anthropogenic activities via long-range transport, the carbon monoxide (Figure 3) and the relative wind direction (Figure 4) respectively have been measured during the considered sampling period. The carbon monoxide (CO) trend showed high values for the beginning of the sampling periods followed by a decrease during the next 10 days with traveling south, most likely due to the crossing of “cleaner” air masses. As the cruise

reached the Hawaii islands, this tendency was interrupted by higher concentration events on May 28th, 29th and June 3rd. This can be due to the influence of anthropogenic activities near the Hawaiian Islands. However, in more polluted air masses, such as near the coast of Japan, CO concentrations can be 3 times higher (up to 400 ppbv, unpublished data) than the average concentrations obtained during our sampling period (112 ± 18 ppbv). Consequently, the results for CO do not show strong influence of anthropogenic activities via long-range transport that could directly affect our Hg measurements. In addition, other gases indicating the influence of urban emissions (such as ethane, propane, and benzene) were measured during the cruise and showed the same trend as CO, with a decrease during the first ten days and low concentrations for the rest of the sampling periods (unpublished data). As for the boat's exhaust stack gases, the wind direction angle, which could lead to contamination, is displayed with $180^\circ \pm 60$ (Figure 4) corresponding to potential of wind blowing from the back of the ship. During the days of May 17th the wind direction pattern shows a potential contamination event as well as two other minor events on May 23rd and 28th. None of these events of wind blowing from the back of the ship affects the RGHg measurements as seen on Figures 4 and 5. However, an important increase in Hg^0 concentrations is observed on May 17th, which could be due to external contaminations, from the boat's exhaust stack gases or other anthropogenic sources (Figure 5).

3.3. Reactive Gaseous, Elemental Mercury and Ozone Chemistry in the MBL

[11] Recent studies have clearly shown that RGHg production, as a result of Hg^0 oxidation, occurs in remote environments, whether in the Arctic or in the marine

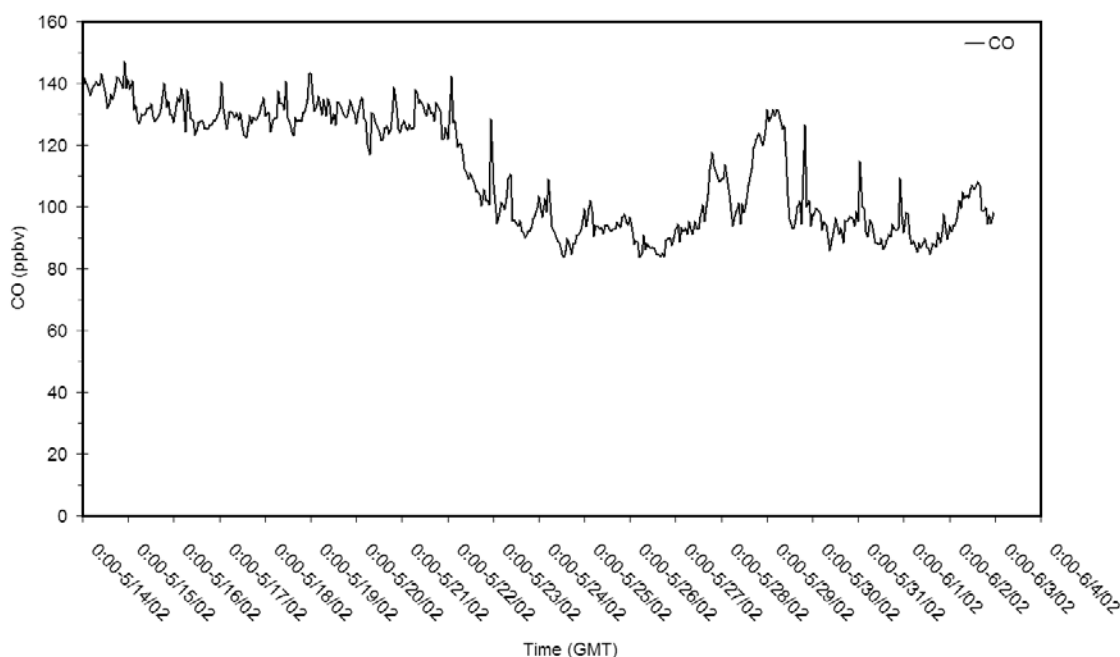


Figure 3. Carbon monoxide (CO) concentration in parts per billion during the sampling period. The measurements were based on a 1-hour step.

boundary layer [Schroeder *et al.*, 1998; Hedgecock and Pirrone, 2001; Hedgecock *et al.*, 2003; Mason and Sheu, 2001; Mason *et al.*, 2001; Lindberg *et al.*, 2002; Lu *et al.*, 2001]. Recently, modeling and experimental studies also confirmed daily variation in RGHg concentrations and the

role of photochemical processes in its production [Hedgecock *et al.*, 2003; Ariya *et al.*, 2002]. Our RGHg data over the North Pacific Ocean show a strong variability in the RGHg concentrations along the cruise track (Figure 5). The RGHg data can be grouped in three distinct temporal periods: the two

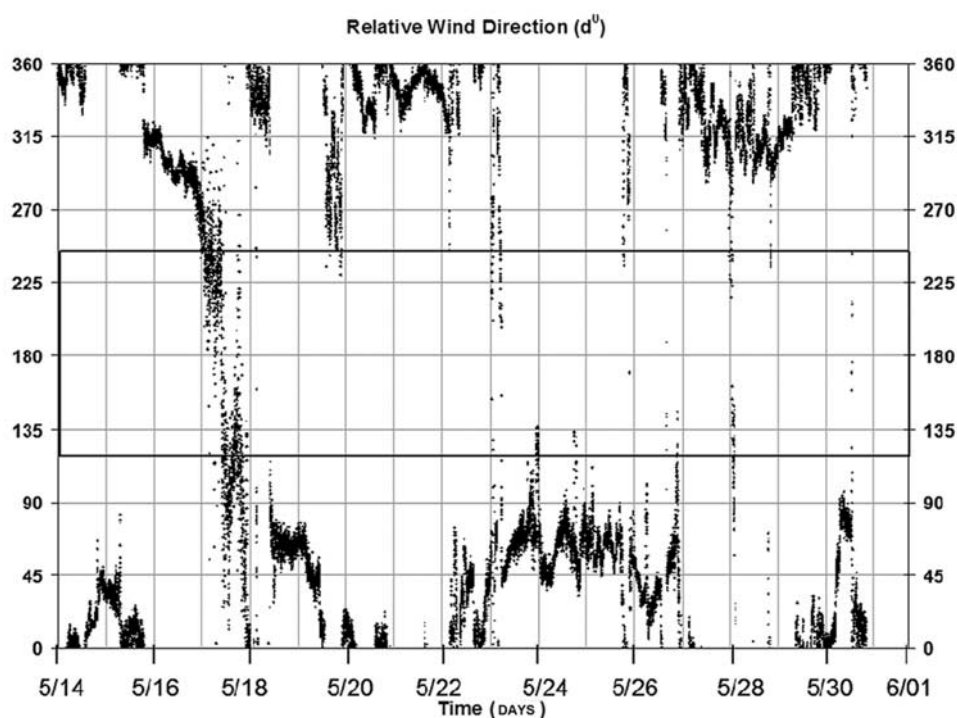


Figure 4. Relative wind direction measured in degree from the front of the ship with 0 and 360 degrees corresponding to the wind blowing from the front of the ship, and 180 degrees to the wind blowing from the back of the ship. The solid-line square corresponds to the zone 180 ± 60 degrees where the exhaust stack gases of the boat could lead to local contamination.

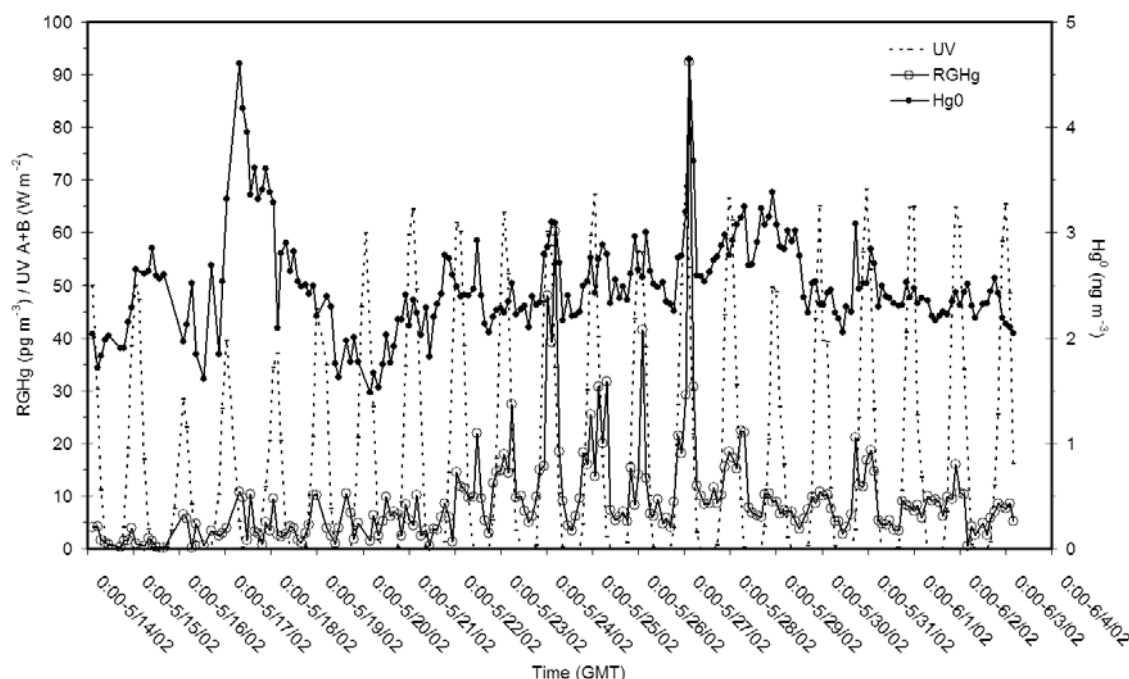


Figure 5. Reactive gaseous mercury (RGHg) and elemental mercury (Hg^0) 2-hourly mean concentrations and ultraviolet radiation (UV) data corresponding to a 2-hour integration, comparable to each RGHg measurement.

first periods are defined similarly as for the ancillary data, one between May 14th and May 21st and the other from May 22nd to May 28th; the third period corresponds to the last week of the cruise. During the first week, at high and middle latitudes, when cold and cloudy weather conditions prevailed, RGHg concentrations displayed very low concentrations and ranged from 0.2 to 10.7 pg m^{-3} , with a mean value of 3.9 pg m^{-3} and with 3.1 pg m^{-3} for standard deviation (\pm). In addition, the very small diurnal cycle is characterized by low midday peaks. For the second week, at low latitudes, when the measurement took place within the tropical waters area, the RGHg concentrations increased (range from 2.8 to 92.4 pg m^{-3} , mean value $13.8 \pm 13.1 \text{ pg m}^{-3}$) and showed more significant diurnal cycle corresponding to the UV pattern, with nocturnal minima and midday RGHg peaks reaching their maximal values for the cruise. Around the Hawaiian Islands, the measurements were also performed under the same tropical conditions; however, RGHg data collected during this third week presented lower concentrations (range from 2.6 to 21.1 pg m^{-3} , mean value $7.8 \pm 3.9 \text{ pg m}^{-3}$) than the previous week. In addition, although the diurnal cycles were significant, the daily variation amplitudes were also smaller than for the previous week. This specific feature was likely due to enhance dry deposition as a result of higher wind speed (see section 3.5).

[12] The atmospheric Hg^0 data reported on Figure 5 corresponded to the 2-hour average of Hg^0 concentrations before each RGHg measurements. Hg^0 concentrations varied from 1.6 to 4.7 ng m^{-3} with an average of $2.5 \pm 0.5 \text{ ng m}^{-3}$. During the first week, the concentrations did not show any significant trend. In addition, the high values have been measured on May 17th, which might be due to external contamination (as discussed above). For the rest of

the cruise, Hg^0 concentrations displayed a similar trend as for RGHg, with an increase within the tropical water. In addition, Hg^0 concentrations also followed a slight diel cycle over the tropical water with higher value measured during the day. In Arctic and Antarctic environments, Hg^0 oxidation and subsequent RGHg formation induced by the polar sunrise, leads to depletion of Hg^0 [Schroeder *et al.*, 1998; Ebinghaus *et al.*, 2002]. On the contrary, such depletion was not observed during our study. Thus, in the MBL and especially in tropical and equatorial MBL, there is a continuous evasional flux of dissolved gaseous mercury (DGHg) from surface water, with the maximal evasion associated with maximal midday UV peak [Mason and Fitzgerald, 1993; Ferrara *et al.*, 2000; Mason *et al.*, 2001]. In addition, our evasional flux calculations (see paragraph 3.6) show that the evaded DGHg can act as a replenishment source of mercury by replacing the depleted Hg^0 and can also account for the daily variation and high values found for Hg^0 concentrations. Consequently, Hg^0 present in the marine boundary layer is, although indirectly, related to photochemical processes since it originates partly from photoreduction in surface water and subsequent evasion.

[13] Overall, our data clearly reinforce the fact that even in the remote MBL, RGHg is present at significant concentrations and that the daily variations in RGHg and Hg^0 concentrations suggest the occurrence of photochemical processes in RGHg formation. These observations are in accordance with those previously reported for the Mediterranean Sea [Sprovieri *et al.*, 2003]. In addition, it appears that RGHg production occurs with a higher efficiency within the tropical marine boundary layer of the North Pacific Ocean compared to higher latitudes. Similar to our

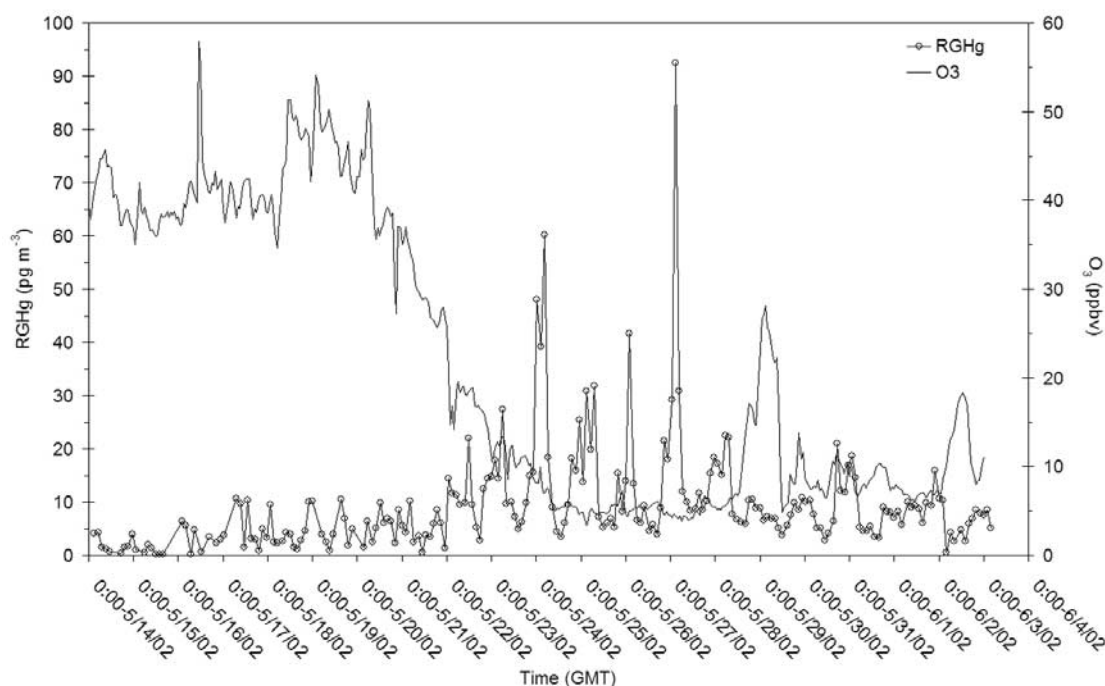


Figure 6. Reactive gaseous mercury (RGHg) 2-hourly mean concentrations and ozone (O_3) 1-hourly mean concentrations (in parts per billion).

measurements collected during the first week, low concentrations of RGHg, without high variation, have been reported for the southern Atlantic Ocean at high latitudes [Temme *et al.*, 2003]. As suggested by Guentzel *et al.* [2001], advection of RGHg from the free troposphere could also account for some of the higher values measured; however, we considered this unlikely as seen by the strong correlation of RGHg with UV and the other photochemically related parameters. Thus, recent studies pointed out the concomitant depletion of ozone (O_3) and Hg^0 in polar environments suggesting interactions of Hg^0 with halogens radicals [Lu *et al.*, 2001; Ebinghaus *et al.*, 2002; Lindberg *et al.*, 2002]. Ozone depletion in the Arctic is believed to be initiated by reactive halogens, most likely bromine oxide (BrO), through the photolysis of gas phase halogen compounds [Barrie *et al.*, 1988; Foster *et al.*, 2001; Bottenheim *et al.*, 2002; Spicer *et al.*, 2002] produced by activation of bromide or chloride from sea-salt aerosol and brine [Finlayson-Pitts *et al.*, 1990; McConnell *et al.*, 1992; Mozurkewich, 1995; Platt and Moortgat, 1999]. In remote MBL [Lal *et al.*, 1998; Dickerson *et al.*, 1999; Galbally *et al.*, 2000; Grant *et al.*, 2000; Shon and Kim, 2002], as well as in polluted midlatitude MBL [Sander and Crutzen, 1996; Hebestreit *et al.*, 1999], variations in O_3 concentrations have also been attributed to reaction with halogen radicals, suggesting an autocatalytic and heterogeneous production of bromine and chlorine [Vogt *et al.*, 1996; Hirokawa *et al.*, 1998; Ayers *et al.*, 1999; Shon and Kim, 2002; von Glasow *et al.*, 2002]. Although direct in situ quantification of bromine activated species are difficult, it is possible to detect their effect by indirect observation based on O_3 variations [Ayers *et al.*, 1999; Nagao *et al.*, 1999; Galbally *et al.*, 2000; Gabriel *et al.*, 2002]. Low O_3 concentrations,

frequently well below 10 ppbv, have been reported by Kley *et al.* [1996] and Singh *et al.* [1996] during aircraft measurements in the marine boundary layer of the tropical Pacific Ocean. In Figure 6, concomitant to the increase in RGHg concentrations, a dramatic decrease in O_3 concentrations (from over 50 to less than 5 ppbv) occurred when the cruise reached the low latitudes suggesting the effect of reactive halogen chemistry on both O_3 depletion and on RGHg formation. To clearly illustrate the role of photochemistry and relationship between O_3 /UV and O_3 /RGHg in the MBL, we plotted (Figure 7) the bihourly mean values of O_3 , UV, RGHg and Hg^0 for two representative days (May 26th and 27th). As shown on Figure 7, the bihourly mean values for ozone decreased significantly (relative decrease of 24%) with a concurrent increase in RGHg and UV. This daily variation in O_3 observed in the tropical area are similar to those pointed out by Nagao *et al.* [1999] which showed a significant O_3 loss in the subtropical MBL of the North Pacific Ocean that occurs just after sunrise and/or during the day, with, once again, halogen chemistry described as a possible mechanism [von Glasow *et al.*, 2002]. The decrease in O_3 with a concomitant increase in UV and RGHg reinforce the hypothesis that even in a remote MBL, RGHg can be produced photochemically with a possible role of ozone and reactive halogens chemistry. Hg^0 appears to be replenished during the most likely as a result photoreduction in surface water and subsequent DGHg evasion (see section 3.6).

3.4. Effect of Environmental and Meteorological Conditions on RGHg Formation

[14] The previously cited studies also showed that the effects of meteorological parameters have a strong impact

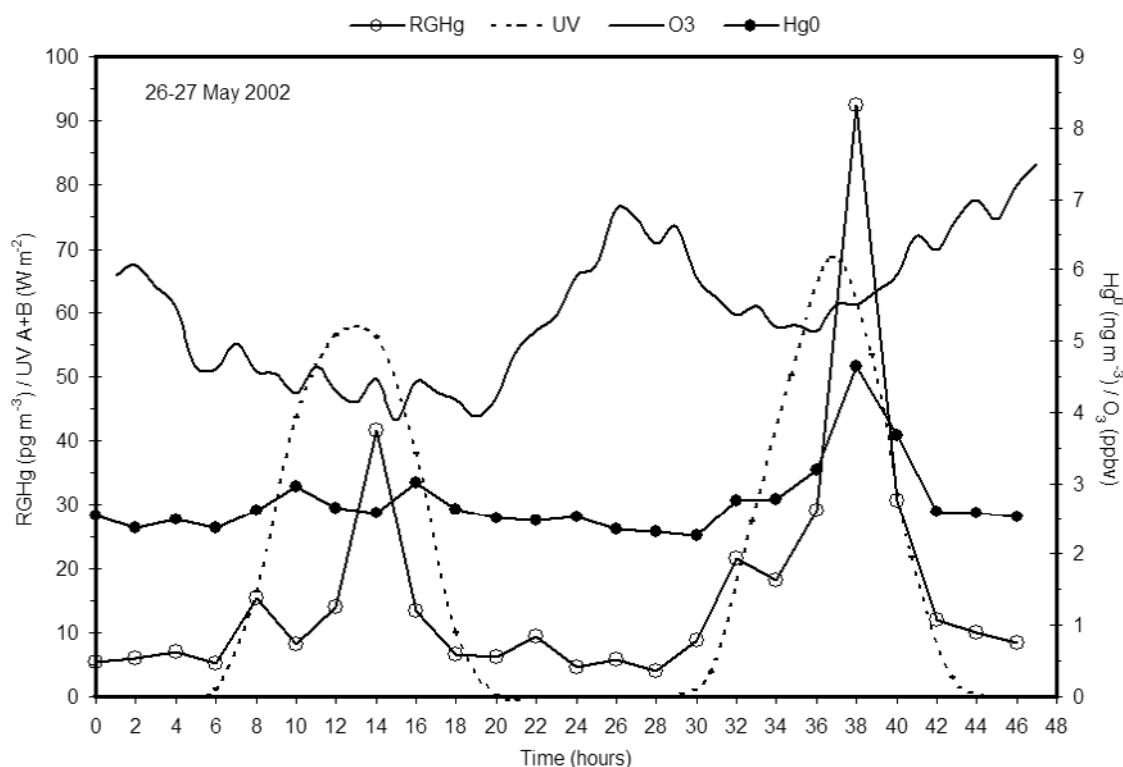


Figure 7. Daily mean value variation for in ozone (O_3), UV, RGHg, and Hg^0 concentrations during a 48-hour time period (May 26th and 27th). The time corresponds to the local standard time expressed in hours (h).

on RGHg concentrations whether in Arctic environment [Lindberg *et al.*, 2002] or in the marine boundary layer [Sprovieri *et al.*, 2003]. Highest RGHg concentrations consistently occurred during periods of reduced wind speed and maximum UV. Thus, the wind speed controls the deposition velocity rates and the removal of RGHg (discussed further in section 3.5) and the photochemistry controls the presence of photochemically induced oxidants: high UV will induce high reactive-oxidant concentrations [Vogt *et al.*, 1996; Dickerson *et al.*, 1999; von Glasow *et al.*, 2002]. Given the high Henry's law constant of RGHg species and consequently its high solubility, the relative humidity and therefore the liquid water content (LWC) of particles in the MBL can lead to a removal of RGHg by wet deposition and a decrease of RGHg in the gas phase [Mason *et al.*, 2001; Hedgecock *et al.*, 2003]. However, high LWC will also influence the sea-salt aerosol concentrations and furthermore the heterogeneous production of the reactive halogens believed to be responsible for Hg^0 oxidation/RGHg formation (as discussed previously). Thus, von Glasow and Sander [2001] showed that pH of sea-salt particles decreases with an increase of relative humidity, leading to the activation and the release of halogens from the sea-salt particles, according to the acid-catalyzed mechanisms discussed by Mozurkewich [1995], Sander and Crutzen [1996], and Vogt *et al.* [1996].

[15] Based on a simple predictive model using local meteorological data, Lindberg *et al.* [2002] showed that in the Arctic, boundary layer entrainment rates and deposition velocities (both modeled as a function of wind speed, UV-B, and air temperature) explained up to $\sim 80\%$ of the measured

variance in RGHg. Since the importance of meteorological factors have been pointed out by the previously cited studies, the different weather conditions during the 2002 IOC cruise could be partly responsible for the differences observed for RGHg concentrations. The low RGHg concentrations (mean value $3.9 \text{ pg m}^{-3} \pm 3.1 \text{ pg m}^{-3}$, Figure 5) measured during the first week were associated either with high relative humidity (daily average 85.5%) but low UV (daily maxima average 41.7 W m^{-2}) due to stormy conditions; or high UV (daily maxima average 62.1 W m^{-2}) but low relative humidity (daily average 66.4%). In addition to these unfavorable conditions in relative humidity and/or UV, the temperature remained cold during this sampling period. As discussed above, in both situations the photochemistry and the production of photochemically induced oxidants could be reduced. During the second and third week, tropical weather conditions prevailed with high temperature (average of $24.6 \text{ d}^\circ\text{C}$), high UV (daily maxima average 62.8 W m^{-2}), and high relative humidity (daily average 80.6%). Assuming that in remote MBL, RGHg production is essentially related to photochemistry [Hedgecock and Pirrone, 2001; Lu *et al.*, 2001; Hedgecock *et al.*, 2003; Mason and Sheu, 2001; Mason *et al.*, 2001; Lindberg *et al.*, 2002; this study], its formation efficiency could be weather reduced or enhanced if associated with unfavorable or favorable photochemistry conditions, respectively.

3.5. RGHg Dry Deposition Velocity, Wet Deposition, and Flux

[16] The effect of wind of RGHg dry deposition can be illustrated by a mass transfer coefficient model. Based on

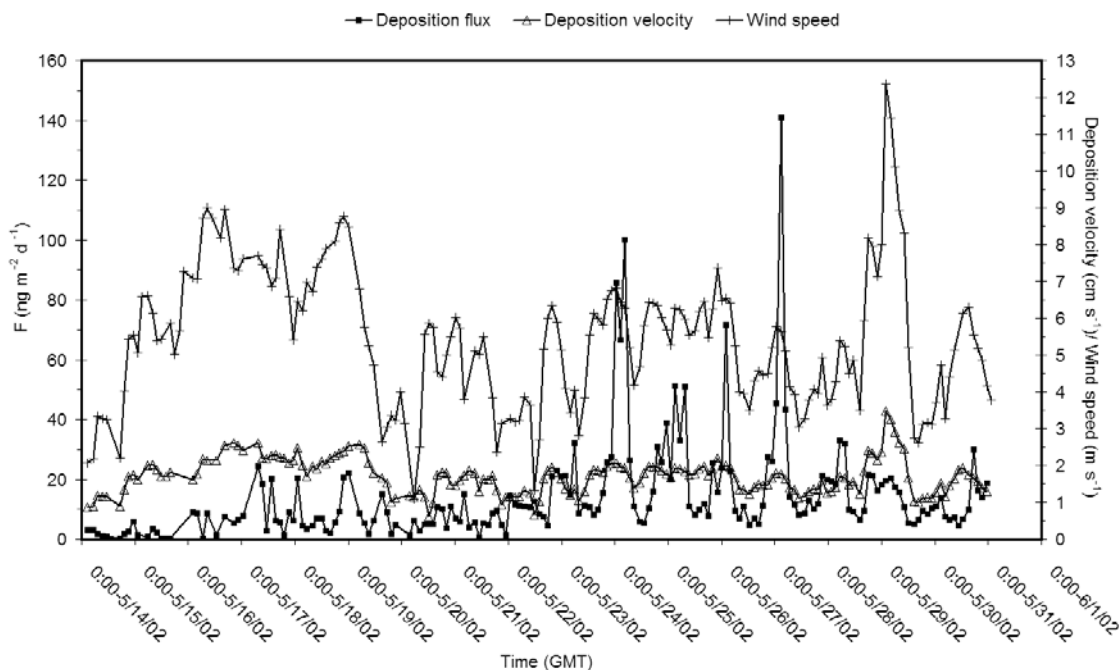


Figure 8. Reactive gaseous mercury (RGHg) bihourly mean dry deposition velocity, flux (F), and true wind speed.

the dry deposition model proposed by *Shahin et al.* [2002], we estimated RGHg dry deposition velocity using

$$k_A = D_A^{0.5}[(0.98 \pm 0.1)u_{10} + (1.26 \pm 0.3)], \quad (1)$$

where k_A is the air-side mass transfer coefficient (cm s^{-1}), D_A is the air-side diffusion coefficient ($\text{cm}^2 \text{s}^{-1}$), u_{10} is the wind speed 10 m above the water surface (m s^{-1}), and the \pm is the 95% confidence interval. We considered for the calculations that RGHg was mainly HgCl_2 . According to *Schwarzenbach et al.* [1993], the air-side diffusion coefficient can be estimated using the liquid molar volume V_m ,

$$D_A = 2.35/(V_m)^{0.73} \quad (2)$$

or alternatively based on the molecular mass m ,

$$D_A = 1.55/(m)^{0.65}. \quad (3)$$

An average of the two diffusion coefficients estimated for HgCl_2 using equations (2) and (3) has been used in the calculation of the dry deposition velocity (1). The dry deposition flux of RGHg can then be easily estimated as

$$F(\text{ng m}^{-2} \text{d}^{-1}) = k_A[\text{RGHg}]. \quad (4)$$

Both RGHg dry deposition velocity and flux are displayed in Figure 8. On average, higher deposition velocities but lower fluxes occurred during the first and beginning of the third weeks compared to the second week (Table 1). High wind speed events (Figure 8) lead to higher deposition velocity and fluxes with a consequent faster removal of RGHg from the MBL. However, in a region of low RGHg production (high latitudes) there will be a low RGHg dry flux. On the

contrary, the tropical area shows very high flux of RGHg dry deposition (up to $141 \text{ ng m}^{-2} \text{d}^{-1}$ or $50 \text{ } \mu\text{g m}^{-2} \text{y}^{-1}$) compared to higher latitudes (average $6.2 \pm 5.8 \text{ ng m}^{-2} \text{d}^{-1}$ or $2.2 \pm 2.1 \text{ } \mu\text{g m}^{-2} \text{y}^{-1}$). In the Hawaiian Islands region, high wind speed induced a faster removal of RGHg by increasing the dry deposition velocity (Figure 8).

[17] The absence of precipitation did not enable us to report wet deposition flux for the first week of the sampling period. However, five events of rain between stations 8 and 9 (Figure 1) were collected and analyzed. The Hg concentrations in rain varied from 6.1 to 29.3 ng l^{-1} and with an average of $14.3 \pm 9.4 \text{ ng l}^{-1}$. The lowest concentrations were typically measured around station 8 (mean value $6.9 \pm 1.6 \text{ ng l}^{-1}$) and the highest for the Hawaiian Islands area, within proximity to Station 9 ($21.6 \pm 7.4 \text{ ng l}^{-1}$). The estimation for Hg wet deposition fluxes (Table 1) were based on Hg concentrations in rain and the monthly total accumulated rainfall for May 2002 over the corresponding surface area (from longitude

Table 1. Mean Calculated Reactive Gaseous Mercury (RGHg) Dry Deposition Velocity and RGHg Dry Deposition, Total Mercury (Hg) Wet Deposition, and Dissolved Gaseous Mercury (DGHg) Evasion Fluxes

	Sampling Period		
	May 14–20	May 21–28	May 29–31
RGHg dry deposition velocity, cm s^{-1}	1.8 ± 0.5^a	1.6 ± 0.3	1.8 ± 0.7
RGHg dry deposition flux, $\text{ng m}^{-2} \text{d}^{-1}$	6.2 ± 5.8	19.9 ± 21.4	12.2 ± 6.3
Hg wet deposition flux, $\text{ng m}^{-2} \text{d}^{-1}$	no data	12.6 ± 9.5	58.3 ± 23.3
DGHg evasion flux, $\text{ng m}^{-2} \text{d}^{-1}$	20.9 ± 18.4	26.0 ± 31.1	59.8 ± 50.3

^aStandard deviation (\pm).

–180 to –150 west and latitude 30 to 15 north). The rainfall data, provided by the Tropical Rainfall Measuring Mission (TRMM) satellite, showed higher rainfall over the Hawaiian Archipelago region (80 to 100 mm) compare to the region including station 8, located between Hawaii and Midway Islands (20 to 40 mm). The relative mercury wet deposition fluxes are consequently higher for the Hawaiian Islands area compared to station 8 vicinity. In addition to the effect of higher wind speed leading to a faster removal of RGHg by dry deposition (as discussed above), higher precipitations could also result in a more efficient removal of RGHg by wet deposition around the Hawaii Islands area and partly explain the lower RGHg concentrations measured in this zone (Figure 5).

3.6. Air-Sea Exchange of Elemental Mercury

[18] As discussed previously, the role of UV intensity could be a key factor in RGHg formation in the boundary layer. In addition, UV strongly influences dissolved gaseous mercury (DGHg) formation by photoreduction of ionic Hg in surface water. Thus, the highest DGHg production, and subsequent evasional flux, occurs when solar radiations are at the maximum [Ferrara *et al.*, 2000; Mason *et al.*, 2001]. Our data show that DGHg concentrations in surface water were significantly ($p < 0.05$) higher in the tropical waters (0.13 ± 0.07 pM) than in the northern latitude waters (0.06 ± 0.03 pM) which characterizes a more efficient photoreduction of the mercury in tropical area. However, the DGHg values are low compared to those measured in the equatorial Pacific Oceans or others oceans surface waters [Mason and Fitzgerald, 1993; Mason *et al.*, 2001].

[19] As we pointed out previously, in Arctic and Antarctic environments, Hg⁰ oxidation, and subsequent RGHg formation induced by the polar sunrise, leads to depletion of Hg⁰ [Schroeder *et al.*, 1998; Ebinghaus *et al.*, 2002], but such depletion was not observed during our study most likely as a result of Hg⁰ replenishment by DGHg evasional flux.

[20] In order to verify these hypotheses, we estimated the evasional fluxes based on the average wind speed, the surface water temperatures, and the gas exchange equation of Wanninkhof [1992], modified for Hg. The waterside exchange coefficient k_w (piston velocity) is

$$k_w (\text{cm h}^{-1}) = 0.31 \hat{u}^2 (\text{Sc}_{\text{Hg}}/\text{Sc}_{\text{CO}_2})^{-0.5},$$

where Sc is the appropriate Schmidt number and \hat{u}^2 is the square of the wind velocity ($\text{m}^2 \text{s}^{-2}$). The evasional flux, F is given by

$$F (\text{ng m}^{-2} \text{d}^{-1}) = k(C_w - C_g/H),$$

where k is the piston velocity in m d^{-1} , C_w is the measured concentration in surface waters (ng m^{-3}), C_g is the measured atmospheric concentration (ng m^{-3}), and H is the dimensionless Henry's law constant, adjusted for temperature and salinity. The calculated DGHg evasion fluxes for each week (corresponding to the three different previously defined sampling areas) are displayed on Table 1. Although variability, the results show that on average the

evasional flux is higher in the tropical water and particularly with high wind speed events, which occurred during the last week (Figure 5). Considering the first 100m of MBL as our measurements took place at 15m above the sea level and based on both DGHg concentrations in the surface water and the corresponding atmospheric Hg⁰ measurements, the estimated evasional flux was equivalent to -0.5 to 53.0% (average of $11.1 \pm 12.2\%$) of the Hg⁰ concentrations. The highest fluxes corresponded to the highest wind speeds (Table 1 and Figure 8). RGHg concentrations represented only from 0.01 to 2% (average $0.4 \pm 0.3\%$) of the corresponding Hg⁰ concentrations. Consequently, evasion from surface water can be considered as a replenishment source of Hg⁰ in the marine boundary layer by replacing the depleted Hg⁰ due to photooxidation. Moreover, the evasional flux can account for the daily variation and high values observed for Hg⁰. Thus, for the second and third week we calculated the Hg⁰ daily relative increase as the difference between daily Hg⁰ minima and maxima and compared the results to DGHg evasional flux. The calculation showed that from 0 up to 134% (mean value $53 \pm 43\%$) of the daily relative increase in Hg⁰ concentrations can be accounted by DGHg evasion from surface water.

[21] On the other hand, although high wind speed enhanced DGHg evasion it also decreases RGHg concentrations by increasing its deposition velocity (as discussed above). The absence of rain did not enable us to estimate a wet deposition flux for the high and middle latitudes; however, in the tropical area mercury dry and wet deposition as well as mercury evasion (Table 1) are in very good accordance with the recent global mercury cycle fluxes estimated by Mason and Sheu [2002].

4. Conclusion

[22] The present study reinforced the hypothesis that RGHg production occurs in remote tropical marine boundary layer, far away from any anthropogenic activities. We also pointed out the importance of the tropical area in the recycling of atmospheric mercury species in the North Pacific Ocean MBL. Moreover, we confirmed that the concentrations in RGHg follow a diel cycle in marine environment and we show that RGHg formation appears to be closely related to photochemically induced processes, particularly those involving heterogeneous reaction, ozone depletion, and reactive halogens chemistry. However, the lack of data concerning halogen radicals over the North Pacific Ocean and their potential interactions with atmospheric mercury species did not allow us to define their exact role in RGHg production. In addition, many different environmental parameters, such as solar radiation, wind speed, and relative humidity, play important roles in the dynamic of mercury in the marine boundary layer, increasing the difficulty to clearly identify all the factors responsible for RGHg formation and cycle over the ocean. Despite the need of further study to improve our understanding in the production of oxidized mercury formation, this study emphasizes the role of the marine boundary layer in the mercury cycling over the ocean. Our data are actually being incorporated into a MBL photochemical model (MOCCA), adapted for mercury [Hedgecock *et al.*, 2003; von Glasow *et*

al., 2002] in order to better estimate the importance of the MBL in the global mercury cycle.

[23] **Acknowledgments.** We would like to thank the Intergovernmental Oceanographic Commission and especially the United States National Science Foundation, Chemical Oceanography, for funding this research (grant OCE-0116925). We also acknowledge the chief scientist (Chris Meyers, University of Hawaii), the captain Dave Murlin, and the crew of the research vessel *Melville* for their support of the 2002 IOC cruise. The rainfall data used in this study were acquired as part of the Tropical Rainfall Measuring Mission (TRMM). The TRMM Science Team developed the algorithms. The data were processed by the TRMM Science Data and Information System (TSDIS) and the TRMM Office; they are archived and distributed by the Goddard Distributed Active Archive Center. TRMM is an international project jointly sponsored by the Japan National Space Development Agency (NASDA) and the U.S. National Aeronautics and Space Administration (NASA) Office of Earth Sciences. This work is a part of an NSF Ocean Sciences funded program.

References

- Ariya, P. A., A. Khalizov, and A. Gidas, Reaction of gaseous mercury with atomic and molecular halogens: Kinetics, products studies, and atmospheric implications, *J. Phys. Chem. A*, **106**, 7310–7320, 2002.
- Ayers, G. P., R. W. Gillett, J. M. Cainey, and A. L. Dick, Chloride and bromide loss from sea-salt particles in the Southern Ocean air, *J. Atmos. Chem.*, **33**, 299–319, 1999.
- Barrie, L. A., and U. Platt, Arctic tropospheric chemistry: An overview, *Tellus*, **49**(5), 450–454, 1997.
- Barrie, L. A., J. W. Bottenheim, P. J. Crutzen, and R. A. Rasmussen, Ozone destruction at polar sunrise in the lower Arctic atmosphere, *Nature*, **334**, 138–141, 1988.
- Bloom, N. S., and W. F. Fitzgerald, Determination of volatile species at the pictogram level by low temperature gas chromatography with cold-vapor atomic fluorescence detection, *Anal. Chim. Acta*, **208**, 151–161, 1988.
- Bottenheim, J. W., J. D. Fuentes, D. W. Tarasick, and K. G. Anlauf, Ozone in the Arctic lower troposphere during winter and spring 2002 (ALERT 2002), *Atmos. Environ.*, **36**, 2535–2544, 2002.
- Bullock, O. R., Modeling assessment of transport and deposition patterns of anthropogenic mercury air emissions in the United States and Canada, *Sci. Total Environ.*, **259**(1–3), 145–157, 2000.
- Bullock, O. R., Jr., W. G. Benjey, and M. H. Keating, Modeling of regional scale atmospheric mercury transport and deposition using RELMAP, in *Atmospheric Deposition of Contaminants to the Great Lakes and Coastal Waters*, edited by J. E. Baker, pp. 323–347, SETAC Press, Pensacola, Fla., 1997.
- Cossa, D., J.-M. Martin, K. Takayanagi, and J. San Juan, The distribution and cycling of mercury species in the western Mediterranean, *Deep Sea Res.*, **44**, 721–740, 1997.
- Cutter, G. A., and C. L. Measures, The 1996 IOC cruise contaminant baseline survey in the Atlantic Ocean from 33°S to 10°N: Introduction, sampling protocols, and hydrographic data, *Deep Sea Res., Part II*, **46**, 867–884, 1999.
- Dickerson, R. R., K. P. Rhoads, T. P. Carsey, S. J. Oltmans, J. P. Burrows, and P. J. Crutzen, Ozone in the remote marine boundary layer: A possible role for halogens, *J. Geophys. Res.*, **104**, 21,385–21,395, 1999.
- Ebinghaus, R., H. H. Knock, C. Temme, J. W. Einax, A. G. Lowe, A. Richter, J. P. Burrows, and W. H. Schroeder, Antarctic springtime depletion of atmospheric mercury, *Environ. Sci. Technol.*, **36**, 1238–1244, 2002.
- Ferrara, R., B. Mazzolai, E. Lanzillotta, E. Nucaro, and N. Pirrone, Temporal trends in gaseous mercury evasion in the Mediterranean seawaters, *Sci. Total Environ.*, **259**, 183–190, 2000.
- Fickert, S., J. W. Adams, and J. N. Crowley, Activation of Br₂ and BrCl via uptake of HOBr onto aqueous salt solutions, *J. Geophys. Res.*, **104**, 24,719–24,727, 1999.
- Finlayson-Pitts, B. J., F. E. Livingston, and H. N. Berko, Ozone destruction and bromine photochemistry at ground level in the Arctic spring, *Nature*, **343**, 622–625, 1990.
- Foster, K. L., R. A. Plastringe, J. W. Bottenheim, P. B. Shepson, B. J. Finlayson-Pitts, and C. W. Spicer, The role of Br₂ and BrCl in surface ozone destruction at polar sunrise, *Science*, **291**, 471–474, 2001.
- Gabriel, R., R. von Glasow, R. Sander, M. O. Andrea, and P. J. Crutzen, Bromide content of sea-salt aerosol particles collected over the Indian Ocean during INDOEX 1999, *J. Geophys. Res.*, **107**(D19), 8032, doi:10.1029/2001JD001133, 2002.
- Galbally, I. E., S. T. Bentley, and C. P. Meyer, Midlatitude marine boundary layer ozone destruction at visible sunrise observed at Cape Grim, Tasmania, 41 degree 5, *Geophys. Res. Lett.*, **27**(23), 3841–3844, 2000.
- Grant, W. B., et al., A case study of transport of tropical marine boundary layer and lower tropospheric air masses to the northern midlatitude upper troposphere, *J. Geophys. Res.*, **105**(D3), 3557–3569, 2000.
- Guentzel, J. L., W. M. Landing, G. A. Gill, and C. D. Pollman, Processes influencing rainfall deposition of mercury in Florida, *Environ. Sci. Technol.*, **35**, 853–873, 2001.
- Hebestreit, K., J. Stutz, D. Rosen, V. Matveiv, M. Pelg, M. Luria, and U. Platt, DOAS measurements of tropospheric bromine oxide in midlatitudes, *Science*, **283**, 55–57, 1999.
- Hedgecock, I. M., and N. Pirrone, Mercury photochemistry in the marine boundary layer—Modeling studies suggest the in situ production of reactive gas phase mercury, *Atmos. Environ.*, **35**, 3055–3062, 2001.
- Hedgecock, I. M., N. Pirrone, F. Sprovieri, and E. Pesenti, Reactive gaseous mercury in the marine boundary layer: Modeling and experimental evidence of its formation in the Mediterranean region, *Atmos. Environ.*, in press, 2003.
- Hirokawa, J., K. Onaka, Y. Kajii, and H. Akimoto, Heterogeneous processes involving sodium halide particles and ozone: Molecular bromine release in the marine boundary layer in the absence of nitrogen oxides, *Geophys. Res. Lett.*, **25**, 2449–2452, 1998.
- Hudson, R. J. M., S. A. Gherini, C. Watras, and D. Porcella, Anthropogenic influences on the global mercury cycle: A model-based analysis, *Water Air Soil Pollut.*, **80**, 265–272, 1995.
- Kim, J. P., and W. F. Fitzgerald, Gaseous mercury profile in the tropical Pacific Ocean, *Geophys. Res. Lett.*, **15**, 40–43, 1988.
- Kley, D., P. J. Crutzen, H. G. J. Smit, H. Vömel, S. J. Oltmans, H. Grassl, and V. Ramanathan, Observations of near-zero ozone concentrations over the convective Pacific: Effect on air chemistry, *Science*, **274**, 230–233, 1996.
- Knipping, E. M., M. J. Lakin, K. L. Foster, P. Jungwirth, D. J. Tobias, R. B. Gerber, D. Dabdub, and B. J. Finlayson-Pitts, Experiments and simulations of ion-enhanced interfacial chemistry on aqueous NaCl aerosols, *Science*, **288**, 301–306, 2000.
- Lal, S., M. Naja, and A. Jayaraman, Ozone in the marine boundary layer over the tropical Indian Ocean, *J. Geophys. Res.*, **103**(D15), 18,907–18,917, 1998.
- Lamborg, C. H., K. R. Rolfhus, W. F. Fitzgerald, and G. Kim, The atmospheric cycling and air-sea exchange of mercury species in the South and equatorial Atlantic, *Deep Sea Res., Part II*, **46**, 957–977, 1999.
- Landis, M. S., R. K. Stevens, F. Shaedlich, and E. M. Prestbo, Development and characterization of an annular denuder methodology for the measurement of divalent inorganic reactive gaseous mercury in ambient air, *Environ. Sci. Technol.*, **36**, 3000–3009, 2002.
- Lin, C., and S. O. Pehkonen, Two-phase model of mercury chemistry in the atmosphere, *Atmos. Environ.*, **32**, 2543–2558, 1998.
- Lin, C., and S. O. Pehkonen, The chemistry of atmospheric mercury: A review, *Atmos. Environ.*, **33**, 2067–2079, 1999a.
- Lin, C., and S. O. Pehkonen, Aqueous phase reactions of mercury with free radicals and chlorine: Implications for atmospheric mercury chemistry, *Chemosphere*, **38**, 1253–1263, 1999b.
- Lindberg, S. E., and W. J. Stratton, Atmospheric mercury speciation: Concentration and behavior of reactive gaseous mercury in ambient air, *Environ. Sci. Technol.*, **32**, 49–57, 1998.
- Lindberg, S. E., S. Brooks, C.-J. Lin, K. J. Scott, M. S. Landis, R. K. Stevens, M. Goodsite, and A. Richter, Dynamic oxidation of gaseous mercury in the arctic troposphere at polar sunrise, *Environ. Sci. Technol.*, **36**, 1245–1256, 2002.
- Lu, J. Y., W. H. Schroeder, L. A. Barrie, and A. Steffen, Magnification of atmospheric mercury deposition to polar regions in springtime: The link to tropospheric ozone depletion chemistry, *Geophys. Res. Lett.*, **28**, 3219–3222, 2001.
- Mason, R. P., and W. F. Fitzgerald, The distribution and biogeochemical cycling of mercury in the equatorial Pacific Ocean, *Deep Sea Res.*, **40**, 1897–1924, 1993.
- Mason, R. P., and G.-R. Sheu, An examination of methods for the measurements of reactive gaseous mercury in the atmosphere, *Environ. Sci. Technol.*, **35**, 1209–1216, 2001.
- Mason, R. P., and G.-R. Sheu, Role of the ocean in the global mercury cycle, *Global Biogeochem. Cycles*, **16**(4), 1093, doi:10.1029/2001GB001440, 2002.
- Mason, R. P., and K. A. Sullivan, Mercury in the South and equatorial Atlantic, *Deep Sea Res., Part II*, **46**, 937–956, 1999.
- Mason, R. P., W. F. Fitzgerald, and F. M. M. Morel, The biogeochemical cycling of elemental mercury: Anthropogenic influences, *Geochim. Cosmochim. Acta*, **58**, 3191–3198, 1994.
- Mason, R. P., K. R. Rolfhus, and W. F. Fitzgerald, Methylated and elemental mercury in the surface and deep ocean waters of the North Atlantic, *Water Air Soil Pollut.*, **80**, 775–787, 1995.
- Mason, R. P., N. M. Lawson, and G.-R. Sheu, Mercury in the Atlantic Ocean: Factors controlling air-sea exchange of mercury and its distri-

- bution in the upper waters, *Deep Sea Res., Part II*, 48, 2829–2853, 2001.
- McConnell, G., S. Henderson, L. Barrie, J. Bottenheim, H. Niki, C. H. Langford, and E. M. Templeton, Photochemical bromine production implicated in Arctic boundary layer ozone depletion, *Nature*, 355, 150–152, 1992.
- Mozurkewich, M., Mechanism for the release of halogens from sea-salt particles by free-radical reactions, *J. Geophys. Res.*, 100, 14,199–14,207, 1995.
- Nagao, I., K. Matsumoto, and H. Tanaka, Sunrise ozone destruction found in the subtropical marine boundary layer, *Geophys. Res. Lett.*, 26, 3377–3380, 1999.
- Nriagu, J. G., and J. M. Pacyna, Quantitative assessment of worldwide contamination of air, water, and soils with trace metals, *Nature*, 333, 134–139, 1988.
- Pai, P., P. Karamchandani, and C. Seigneur, Simulation of the regional atmospheric transport and fate of mercury using a comprehensive eulerian model, *Atmos. Environ.*, 31(17), 2717–2732, 1997.
- Platt, U., and G. K. Moortgat, Heterogeneous and homogeneous chemistry of reactive halogen compounds in the lower troposphere, *J. Atmos. Chem.*, 34, 1–8, 1999.
- Pleijel, K., and J. Munthe, Modeling the atmospheric mercury cycle—Chemistry in fog droplet, *Atmos. Environ.*, 29, 1441–1457, 1995.
- Porcella, D. B., C. Ramel, and A. Jernelov, Global mercury pollution and the role of gold mining: An overview, *Water Air Soil Pollut.*, 97, 205–207, 1997.
- Sander, R., and P. J. Crutzen, Model study indicating halogen activation and ozone destruction in polluted air masses transported to the sea, *J. Geophys. Res.*, 101, 9121–9138, 1996.
- Sander, R., Y. Rudlich, R. von Glasow, and P. J. Crutzen, The role of BrNO₃ in the marine tropospheric chemistry: A model study, *Geophys. Res. Lett.*, 26, 2857–2860, 1999.
- Schroeder, W. H., and J. Munthe, Atmospheric mercury—An overview, *Atmos. Environ.*, 32, 809–822, 1998.
- Schroeder, W. H., K. G. Anlauf, L. A. Barrie, J. Y. Lu, A. Steffen, D. R. Schneeberger, and T. Berg, Arctic springtime depletion of mercury, *Nature*, 394, 331–333, 1998.
- Schwarzenbach, R. P., P. M. Gschend, and D. M. Imboden, Molecular diffusivities, in *Environmental Organic Chemistry*, pp. 194–200, Wiley-Interscience, Hoboken, N. J., 1993.
- Shahin, U. M., T. M. Holsen, and M. Odabasi, Dry deposition with a surface water surface sampler: A comparison to modeled results, *Atmos. Environ.*, 36, 3267–3276, 2002.
- Sheu, G.-R., and R. P. Mason, An examination of the methods for the measurement of reactive gaseous mercury in the atmosphere, *Environ. Sci. Technol.*, 35, 1209–1216, 2001.
- Sheu, G.-R., R. P. Mason, and N. M. Lawson, The speciation and distribution of atmospheric mercury over the northern Chesapeake bay, in *Chemicals in the Environment: Fate, Impacts, and Remediation, ACS Symp. Ser.*, vol. 806, edited by R. L. Lipnick et al., pp. 223–242, Am. Chem. Soc., Washington, D. C., 2002.
- Shia, R.-L., C. Seigneur, P. Pai, M. Ko, and N.-D. Sze, Global simulation of atmospheric mercury concentrations and deposition fluxes, *J. Geophys. Res.*, 104, 23,747–23,760, 1999.
- Shon, Z.-H., and N. Kim, A modeling study of halogen chemistry's role in marine boundary layer ozone, *Atmos. Environ.*, 36, 4289–4298, 2002.
- Singh, H. B., et al., Low ozone in the marine boundary layer of the tropical Pacific Ocean: Photochemical loss, chlorine atoms, and entrainment, *J. Geophys. Res.*, 101, 1907–1917, 1996.
- Spicer, C. W., R. A. Plastring, K. L. Foster, J. Finlayson-Pitts, J. W. Bottenheim, A. M. Grannas, and P. B. Shepson, Molecular halogens before and during ozone depletion events in the Arctic at polar sunrise: Concentrations and sources, *Atmos. Environ.*, 36, 2721–2731, 2002.
- Sprovier, F., N. Pirrone, and J. Sommar, Mercury speciation in the marine boundary layer along a 6000 km cruise path around the Mediterranean Sea, *Atmos. Environ.*, in press, 2003.
- Temme, C., J. W. Einax, R. Ebinghaus, and W. H. Schroeder, Measurements of atmospheric mercury species at a coastal site in the Antarctic and over the South Atlantic Ocean during polar summer, *Environ. Sci. Technol.*, 37, 22–31, 2003.
- Vogt, R., P. J. Crutzen, and R. Sander, A mechanism for halogen release from sea salt aerosol in the remote marine boundary layer, *Nature*, 383, 327–330, 1996.
- von Glasow, R., and R. Sander, Variation on sea-salt aerosol pH with relative humidity, *Geophys. Res. Lett.*, 28, 247–250, 2001.
- von Glasow, R., R. Sander, A. Bott, and P. J. Crutzen, Modeling halogen chemistry in the marine boundary layer: I. Cloud-free MBL, *J. Geophys. Res.*, 107(D17), 4341, doi:10.1029/2001JD000942, 2002.
- Wanninkhof, R., Relationship between wind speed and gas exchange over the ocean, *J. Geophys. Res.*, 97(C5), 7373–7382, 1992.
- Xu, X., X. Yang, D. R. Miller, J. J. Helble, and R. J. Carley, A regional scale modeling study of atmospheric transport and transformation of mercury. II. Simulation results for the northeast United State, *Atmos. Environ.*, 34(28), 4945–4955, 2000.

S. Kato, Department of Applied Chemistry, Tokyo Metropolitan University, 192-0397 Tokyo, Japan.

F. J. G. Laurier, R. P. Mason, and L. Whalin, Chesapeake Biological Laboratory, University of Maryland, Solomons, MD 20688, USA. (laurier@cbl.umces.edu)